Plasma Phys. Control. Fusion 60 (2018) 024003 (7pp) https://doi.org/10.1088/1361-6587/aa9d27

# Evolution of plasma wakes in density up- and down-ramps

C J Zhang[1], C Joshi[1], X L Xu[1], W B Mori[1], F Li[2], Y Wan[2], J F Hua[2], C H Pai[2], J Wang[3] and W Lu[2]

[1] University of California Los Angeles, Los Angeles, CA 90095, United States of America
[2] Department of Engineering Physics, Tsinghua University, Beijing 100084, People's Republic of China
[3] Institute of Atomic and Molecular Sciences, Academia Sinica, Taipei 10617, Taiwan

E-mail: jfhua@tsinghua.edu.cn

Received 10 October 2017, revised 22 November 2017
Accepted for publication 24 November 2017
Published 3 January 2018

**Abstract**

The time evolution of plasma wakes in density up- and down-ramps is examined through theory and particle-in-cell simulations. Motivated by observation of the reversal of a linear plasma wake in a plasma density upramp in a recent experiment (Zhang *et al* 2017 *Phys. Rev. Lett.* **119** 064801) we have examined the behaviour of wakes in plasma ramps that always accompany any plasma source used for plasma-based acceleration. In the up-ramp case it is found that, after the passage of the drive pulse, the wavnumber/wavelength of the wake starts to decrease/increase with time until it eventually tends to zero/infinity, then the wake reverses its propagation direction and the wavenunber/wavelength of the wake begins to increase/shrink. The evolutions of the wavenumber and the phase velocity of the wake as functions of time are shown to be significantly different in the up-ramp and the down-ramp cases. In the latter case the wavenumber of the wake at a particular position in the ramp increases until the wake is eventually damped. It is also shown that the waveform of the wake at a particular time after being excited can be precisely controlled by tuning the initial plasma density profile, which may enable a new type of plasma-based ultrafast optics.

Keywords: plasma wake evolution, density ramps, wake reversal, plasma-base photonic device

(Some figures may appear in colour only in the online journal)

## 1. Introduction

When a short but intense laser pulse or a charged particle beam propagates in a plasma, the ponderomotive force of the laser pulse or the Coulomb force of the charged particle beam will push the plasma electrons away from their equilibrium positions to set up oscillations [1, 2]. These oscillations form a wave or a wake that follows the drive pulse with its phase velocity equals to the group velocity of the drive pulse. The wake has intense electric fields with amplitudes that are orders of magnitude larger than that of the conventional radio-frequency based accelerators. These fields can be utilized to accelerate electrons [3–7] or positrons [8, 9] to high energy within a much shorter distance compared to the conventional accelerators. This unique characteristic of plasma-based accelerators (PBA) opens a lot of new opportunities including building extremely compact modest-energy accelerators and developing PBA-based light sources [10–13]. It also provides a possible new paradigm for building the next-generation colliders [14].

A recent experiment [15] showed that the plasma wakes evolve in an unexpected way in a plasma density up-ramp, i.e., the wavelength of the wake at a particular position initially increases with time to infinity and then decreases and the wake eventually reverses its propagation direction. This phenomenon originates from simple plasma physics but had not been observed in practice. This spatio-temporal wake behaviour is different in plasma density up-ramp versus down-ramp. The evolution of wakes in inhomogeneous plasmas is also relevant to wakefield emission. For example, it was proposed to shoot an intense laser obliquely into an inhomogeneous plasma with an angle between the wave vector and the density gradient to generate intense terahertz (THz) emissions through linear mode conversion [16].

 

Furthermore, the fast evolution of the wavelength of the plasma wake could possibly be used as a new type of plasma photonic device.

In this paper, the evolution of plasma wakes in a density up-ramp is studied analytically and by particle-in-cell (PIC) simulations. This same framework has been used to explain the direct spatio-temporal observations of a laser-induced linear wake in a recent experiment [15]. It is shown that the wavenumber of the wake indeed decreases with time in a density up-ramp. This evolution of wavenumber at a given point in space originates from the phase mixing of plasma oscillations at both lower and higher density on either side of that location. In a density up-ramp, the wavenumber of the wake decreases to zero when plasma electrons everywhere in space come into phase. As they begin to dephase, the phase velocity of the wake changes its direction and starts to propagate backwards. Therefore, we call this phenomenon plasma wake reversal. As a result of the change of wavenumber, the wavelength of the wake initially increases with time until it becomes infinity and then starts to shrink until it can be damped by wave-particle interactions. The phase velocity of the wake evolves in a similar way as the wavelength does—firstly increasing to infinity and then begins to decrease. The situation of wake evolution in a plasma density down-ramp is quite different and is also presented here for completeness. Since the evolution of the wake depends on the local density gradient, an example of controlling the evolution process of the wake by tuning the initial density profile is given. Examples of how nonlinear wakes evolve in plasma density upramps are also presented.

## 2. Theory

The drive pulse is assumed to pass through the plasma density ramp at nearly the speed of light $c$ and create a wake. Since the group velocity of the wake is almost zero, the plasma electrons keep oscillating around their equilibrium positions with the local plasma frequency long after the drive pulse has passed through the plasma. The electrons at different longitudinal locations can be modelled as a series of oscillators. Those oscillators have a certain initial phase which can be written as

$$\phi(z, t) = \omega_p(z)(t - z/v_d), \tag{1}$$

where $\omega_p(z) = \sqrt{n_e(z)e^2/\epsilon_0 m_e}$ is the local plasma frequency and $v_d \approx c$ is the group velocity of the drive laser pulse. The dependence of $v_d$ on $\omega_p(z)$ is a higher order effect that is usually negligible. Consequently, the frequency and the wavenumber of the wake can be written as $\omega(z, t) \equiv \partial\phi/\partial t = \omega_p(z)$ and $k(z, t) \equiv -\partial\phi/\partial z = k_p(z) - \frac{\partial\omega_p}{\partial z}t$, respectively. These two equations imply that the wavenumber of the plasma wake evolves in time according to

$$\frac{\partial k}{\partial t} = -\frac{\partial\omega_p}{\partial z}. \tag{2}$$

Equation (2) indicates that the evolution of the wavenumber of the wake depends on the local frequency (density) gradient. For a position where the local frequency gradient is zero, the wavenumber of the wake remains constant. However, for the up-ramp case, $\partial\omega_p/\partial z > 0$, which means $\partial k/\partial t < 0$ therefore the wavenumber of the wake everywhere will decrease with time. This also means that the wavelength of the wake initially increases with time and will become infinity after a certain period of time when the wavenumber goes to zero. After that, the wavenumber keeps decreasing but its amplitude increases because now the wavenumber has become negative and the wake has reversed its propagation direction. The wake wavelength now starts to shrink until the wake can be eventually damped. For the down-ramp case, $\partial\omega_p/\partial z < 0$, which means $\partial k/\partial t > 0$ therefore the wavenumber of the wake will keep increasing with time. As a result, the wavelength of the wake will monotonically decrease (and the phase velocity will decrease from $c$ to eventually close to the thermal velocity $v_{\text{th}}$) until the wake can be damped.

The phase velocity of the wake is calculated as

$$v_\phi(z, t) \equiv \frac{\omega}{k} = v_d\left(1 - \frac{v_d}{\omega_p(z)}\frac{\partial\omega_p(z)}{\partial z}t\right)^{-1}. \tag{3}$$

It can be seen that in a homogeneous plasma ($\partial\omega_p/\partial z = 0$), the phase velocity of the wake always equal to the group velocity of the drive pulse as expected. However, for the up-ramp and down-ramp cases, the phase velocity equals to the group velocity of the driver is only true for $t = 0$. For the up-ramp case, after being excited, the wake's phase velocity increases with time to infinity at $t = \frac{\omega_p(z)}{v_d}\Big/\frac{\partial\omega_p(z)}{\partial z}$, then reverses its sign to minus infinity and keeps increasing to zero. For the down-ramp case, the phase velocity of the wake decreases monotonically to zero. Unlike in the up-ramp case, now the phase velocity decreases to half of its initial value at $t = \frac{\omega_p(z)}{v_d}\Big/\frac{\partial\omega_p(z)}{\partial z}$.

Since the evolution of $k$ depends on the local density gradient, we can control how the wavenumber (hence the wavelength) evolves by tuning the initial density profile. For example, by letting $k(z, t_a) = \alpha$, we can find a solution for the initial plasma density profile

$$n_e(z) = \frac{m_e\epsilon_0}{e^2}(c\alpha + \beta e^{z/ct_a})^2, \tag{4}$$

where $v_d$ has been replaced by $c$ for clarity. Here $\alpha$ and $\beta$ are constants. For a given $\alpha$, a series of density profiles (corresponding to different $\beta$) can be found where the wakes evolve to a state with the same wavelength for all different $z$ locations at the same time $t = t_a$. That means although the initial wavelength is different due to the non-uniform density profile, the wavelength evolves to be the same ($\lambda = 2\pi/\alpha$) for all $z$ positions at some later time $t_a$.

## 3. Simulations

In this section, we present PIC simulations carried out using the OSIRIS code [17]. To save time and computational resources, 2D geometry and electron beam drivers were used in all simulations. A typical simulation box has dimensions of $9480 \times 400\, c/\omega_0$ in the direction of parallel- and perpendicular to the driver propagation direction, where $\omega_0 = 2\pi\, c/\lambda_0$ is the angular frequency and $\lambda_0$ is the wavelength of the drive laser. In all simulations presented in this paper, we have chosen $\lambda_0 = 800$ nm as a reference. The simulation box was divided into $1640 \times 400$ cells. Pre-ionized plasmas with mobile helium ions were used in these simulations. The plasma density rises from zero at $z = 800\, c/\omega_0$ to $7.5 \times 10^{16}\,\mathrm{cm}^{-3}$ at $z = 1200\, c/\omega_0$ with a $\sin^2$ profile. The density keeps rising to $1.05 \times 10^{17}\,\mathrm{cm}^{-3}$ at $z = 9840\, c/\omega_0$ with another $\sin^2$ profile. An electron beam driver with a bi-Gaussian density profile ($\sigma_z = 12.7\ \mu$m, $\sigma_r = 15\ \mu$m, centred at $z = 400\, c/\omega_0$) was used to excite a linear wake (the peak density of the driver $n_b = 4.7 \times 10^{15}\,\mathrm{cm}^{-3}$ is much smaller than the plasma density) in the relatively low-density plasma. For all three species (plasma electrons, ions and the driver electrons), $2 \times 2$ particles with quadratic shape were initialized in each cell. Absorbing boundary conditions for both the electromagnetic fields and the particles were used for all directions.

### 3.1. Wake wavenumber evolution

The simulation results are shown in figure 1 for the up-ramp case (a) and the down-ramp case (b), respectively. The density profiles used in these simulations are shown by the red lines in the top frames. The profile of these ramps is described in the above paragraph. The bottom frames in each column show the correspondingly longitudinal electric fields for different elapsed time. In both cases, the linear wake (maximum $n_1/n_0$ is $\sim$8%, $n_1$ is the amplitude of density perturbation and $n_0$ is the initial density) initially propagates from left to right as indicated by the black arrows in the second-row frames. As explained in the theory section, the wavelength of the wake firstly increases then decreases in the up-ramp case whereas it keeps shrinking in the down-ramp case. It can also be seen clearly from both columns that the wake wavelength evolves with time in a different way at different $z$ positions due to the correspondingly different density gradients.

To quantitatively compare the simulation results with the theory, evolutions of the wavenumber at $z = 700\ \mu$m, as functions of time are plotted in figure 2. The red and blue lines are theoretical predictions calculated using the initial $k(t = 0)$ and $\frac{\partial k}{\partial t}|_{t=0}$ for the up-ramp and down-ramp cases, respectively. The squares and circles are the corresponding simulation results. Both the calculations and the simulation results are taken at $z = 700\ \mu$m. Note that what is plotted in figure 2 is the absolute value of $k$. The red line decreases to zero at $t \approx 13$ ps which means that at this time the wake wavelength becomes infinity and the wake reverses its propagation direction as can be seen in figure 1(a).

### 3.2. Phase velocity evolution

The phase velocity of the wake also evolves with time due to the evolution of the wavenumber since the frequency does not change. Therefore, a decrease (increase) of the wavenumber implies an increase (decrease) of the phase velocity. In the up-ramp case, the phase velocity will increase initially until it goes to infinity at $t = \frac{\omega_p(z)}{v_d} \Big/ \frac{\partial \omega_p(z)}{\partial z}$; then the wake reverses its propagation direction and the phase velocity decreases eventually to zero. In the down-ramp case, the phase velocity decreases monotonically to zero.

The phase velocity of the wake can be calculated using equation (3). For example, for the density profile shown in figure 1(a), the phase velocity at $z = 700\ \mu$m is calculated to be $v_\phi(t) = c/(1 - 0.075t\,[\mathrm{ps}])$ where the approximation $v_d \approx c$ has been made. For the up-ramp case, this function is plotted as the red line in figure 3. The calculated phase velocity shows an expected behaviour: it firstly increases with time and then decreases to zero. The dashed line marks the time when the phase velocity becomes infinity also as expected. The open circles in figure 3 are simulation results, which show an excellent agreement with the calculations. For the down-ramp case (blue line and circles) the phase velocity monotonically decrease from $c$ towards zero as expected. However, such a decrease happens at every $z$ location as a function of time is a result of phase mixing of high-frequency plasma oscillations, which is different from the phase velocity decrease as a function of $z$ location when the driver propagates through the down-ramp.

### 3.3. Phase space evolution

In both the up-ramp and down-ramp cases, the phase velocity of the wake eventually decreases to much slower than the speed of light, which means the wake can eventually interact with thermal plasma electrons and be damped through Landau damping [18]. This is verified by checking the phase space of the electrons. In figure 4, we plot the longitudinal ($z - p_z$) phase space of electrons. The electrons shown here are selected according to their coordinates: $0.2 < z < 1.2$ mm and $-15 < y < 15\ \mu$m. Note that the initial temperature of the plasma is set to zero in the simulation.

Once again, the evolution of the wavelength of the wake can be clearly seen. The electrons in the middle of the window move in a collective behaviour at early time as shown in figures 4(a) and (b). Later on, as the phase velocity of the wake slows down, some electrons are trapped and gain/lose energy from the wakefield. However, since the phase velocity of the wake continues decreasing and the wavelength of the wake keeps shrinking as a result of phase mixing of high-frequency oscillations, the trapped electrons will sample the accelerating and decelerating phase in an oscillating way thus they cannot be continuously accelerated in the normal wakefield acceleration sense. The electrons are rather finally thermalized instead of being accelerated. The energy stored in the wakefield excited by the driver is eventually converted to the thermal energy of the plasma.

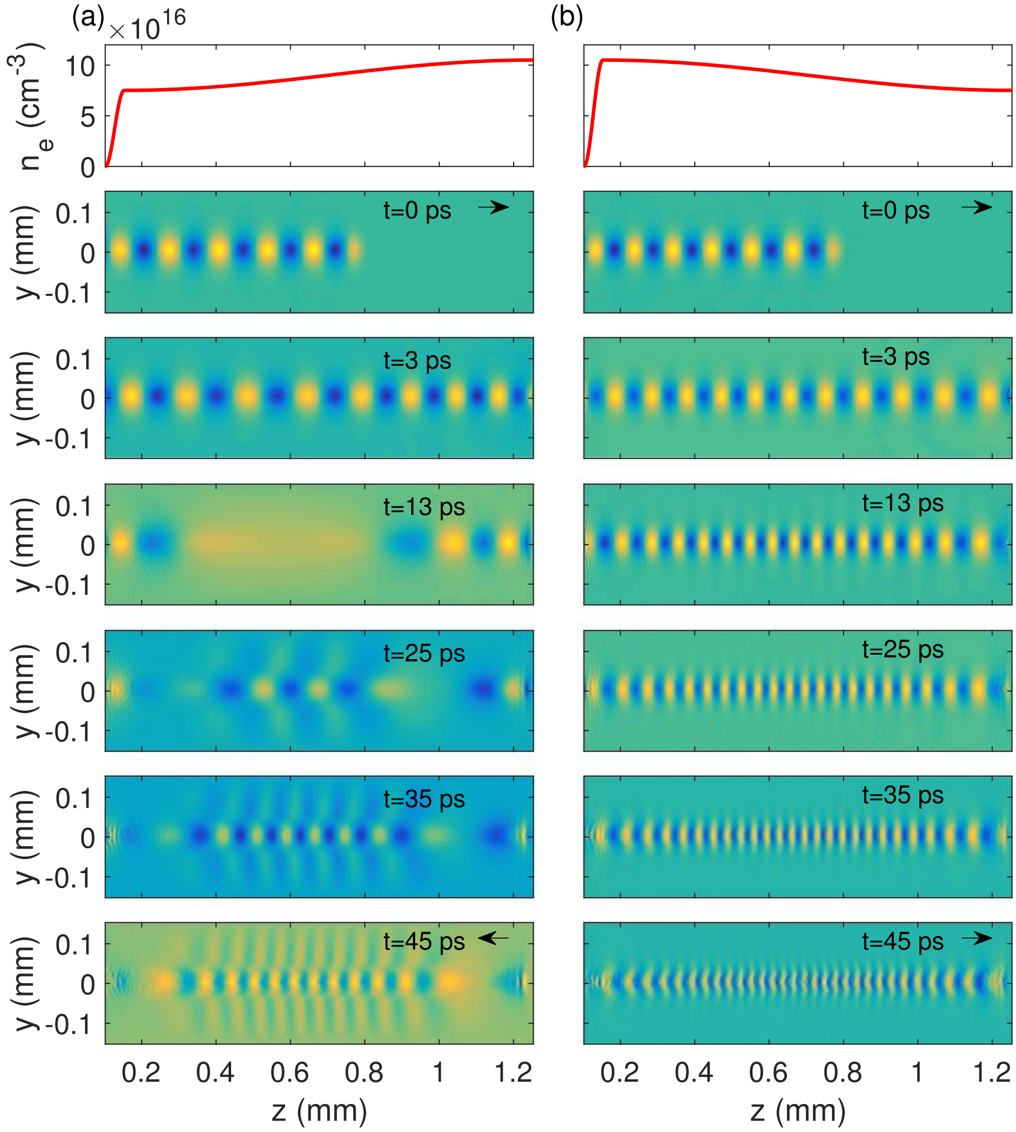


**Figure 1.** Left column (a), the plasma density profile used in the simulation (top frame) and longitudinal fields for different elapsed time for the up-ramp case. Right column (b), the plasma density profile used in the simulation (top frame) and longitudinal fields for different elapsed time for the down-ramp case. The colour tables in all the shots have been adjusted to highlight the wake wavelength variation.

### *3.4. Controlling the wake evolution dynamics*

As explained in the foregoing section, the evolution of wake wavenumber as a function of time can be controlled by initializing different density profiles. For example, wavelength of the wake in a density profile given by equation (4) will evolve to be the same for all different $z$ locations at time $t = t_a$. And this particular wavelength is $\lambda = 2\pi/\alpha$ thus can be controlled by changing $\alpha$. Three different plasma density profiles are plotted in figure 5(a), which correspond to the same $\alpha = 0.01\pi\ \mu\mathrm{m}^{-1}$ but different $\beta$ (7.1, 9.4 and 11.8 $\mathrm{ps}^{-1}$ for the blue, green and red line, respectively). The correspondingly initial waveforms (axial lineout of the $E_z$ field) are shown in figures 5(b)–(d). Because the density profiles are different, the initial wavelength also differ from one other. However, the wavelength in all three cases become the same at $t = t_a$ (in this example $t_a = 5$ ps) as can be seen in figures 5(e)–(g). Furthermore, the wavelength equals to $2\pi/\alpha = 200\ \mu\mathrm{m}$ which agrees very well with the theoretical prediction. This controllable feature of the wake evolutions may enable a new type of plasma-based ultrafast photonic device—a spatially chirped dynamic phase-grating. Due to their fast-evolving feature, the modulated density structure (or the electric field structure) of the wake can be used to time-dependently diffract photon beams (or electron beams).

### *3.5. Nonlinear wake evolution*

Results presented above are based on the linear theory. If we increase the peak density of the beam driver (or the intensity of the laser driver), the wake will become nonlinear. Therefore the oscillation frequency will depend on the amplitude, which may introduce nonlinearity into the aforementioned simple relation between $\partial k/\partial t$ and $\partial \omega_p/\partial z$. To illustrate this, simulations with $n_b = 0.4$, 1, 2, $3n_p$ were carried out and the snapshots of $E_z$ fields after different elapsed time are plotted

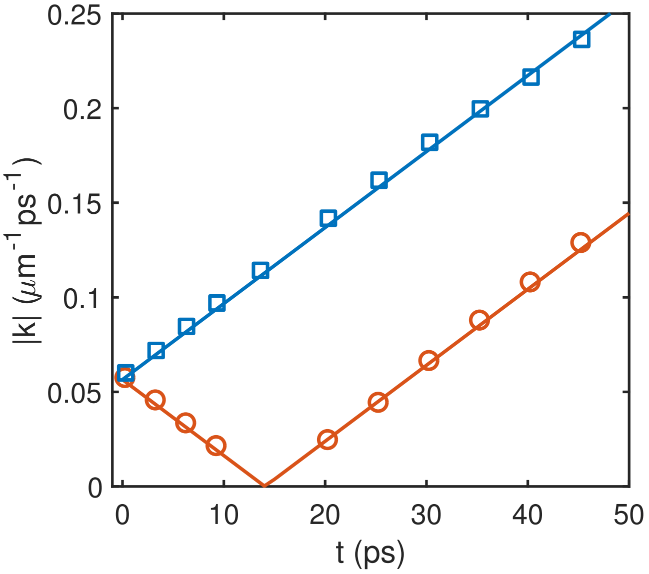


**Figure 2.** Wavenumber of the wake changes as a function of time. The red and blue lines are calculations for the up-ramp and down-ramp case, respectively. Squares and circles are the corresponding simulation results taken at $z = 700\ \mu$m.

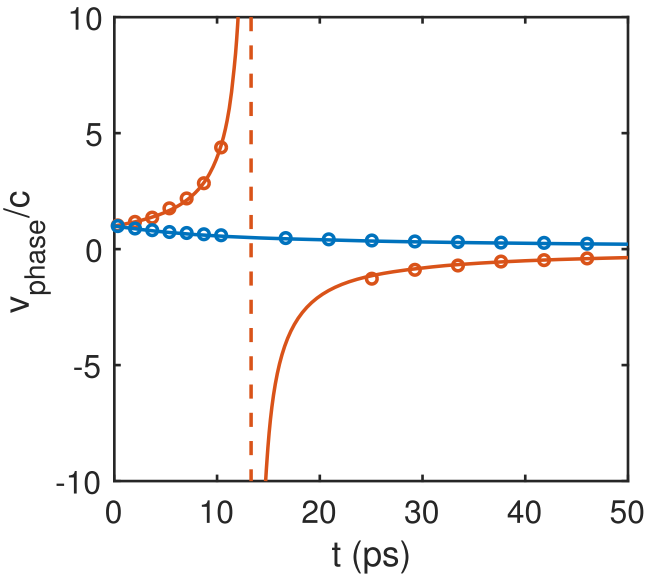


**Figure 3.** Calculated (line) and simulated (open circles) phase velocity of the wake. The dashed line marks the position where the phase velocity becomes infinity. Both the calculation and the simulation are made using parameters at $z = 700\ \mu$m where the density gradient reaches maximum.

in figure 6. The normalized charge per unit length $\Lambda \equiv \int_0^\infty r n_b \mathrm{d}r$ for these drivers are 0.3, 0.7, 1.4 and 2.2, respectively. The left column shows the results for the $n_b = 0.4 n_p$ case. It can be seen that although the wake still evolves in a similar way as that in the linear case at earlier time, there appears some smaller wavelength modulations after the wake reverses its propagation direction. The on-axis portion of the wake smeared out more rapidly than that in the linear case. After the on-axis portion of the wake has disappeared, there exist wakes beside the on-axis portion

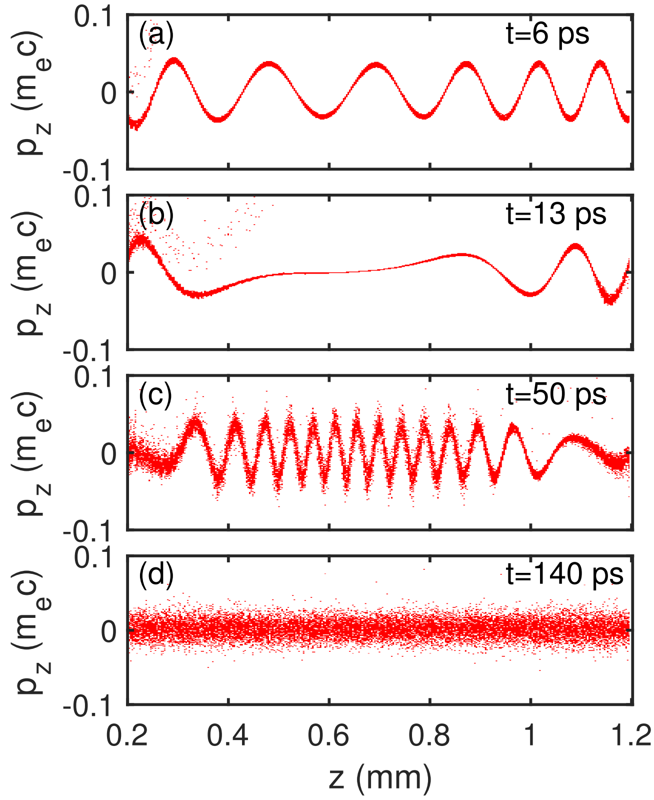


**Figure 4.** Longitudinal phase spaces at four different times.

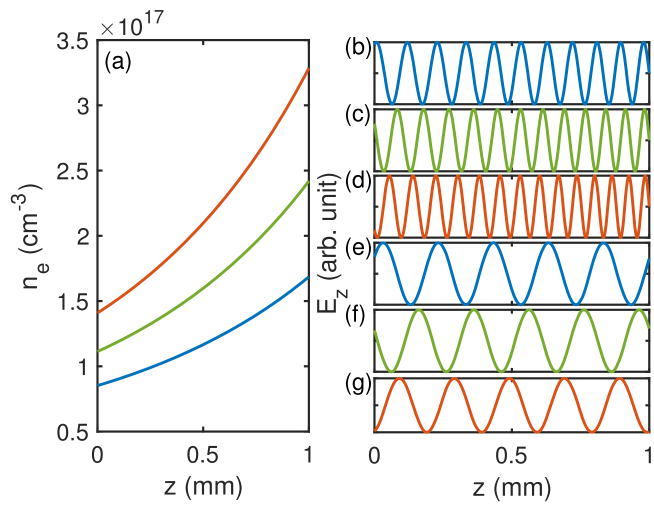


**Figure 5.** (a) Different initial plasma density profiles with $\beta = 7.06$ ps$^{-1}$ (blue), 9.42 ps$^{-1}$ (green) and 11.77 ps$^{-1}$ (red). $\alpha = 0.01\pi\ \mu$m$^{-1}$ for all three cases. (b)–(d) show the correspondingly initial axial lineouts of the wakefield; (e)–(g) show the correspondingly axial lineouts of the wakefield at $t = t_a$.

forming a hollow cylinder structure of wakes. In the other three columns, the initial wakes are more and more nonlinear, which makes the wakes undergo more complex evolutions. An interesting phenomenon is that in the $n_b = 2n_p$ case, a ring structure of the electric fields forms after the wake has completely disappeared as can be seen in the last two frames in the third column.

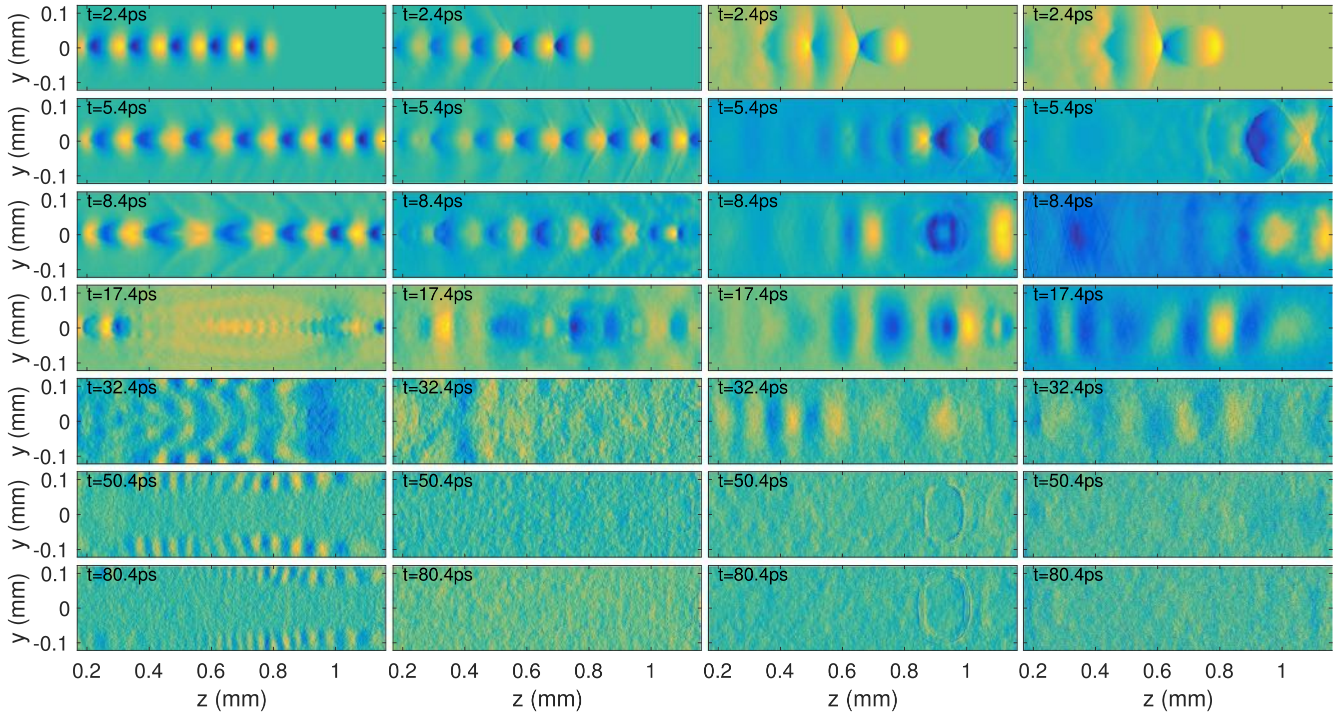


**Figure 6.** Accelerating electric fields of four different simulations with different driver density. From the left to the right column, $n_b = 0.4$, 1, 2, $3n_p$ respectively. The colour tables in all the shots have been adjusted to highlight the wake wavelength variation.

## 4. Conclusion

The evolutions of plasma wake in a density up-ramp or a down-ramp are studied theoretically and by PIC simulations. The evolution of the wavenumber shows different behaviour in the two cases. In the up-ramp case, the wavenumber of the wake decreases with time whereas in a down-ramp case the wavenumber keeps increasing. After the wavenumber decreases to zero in the up-ramp case, the wake reverses its direction and propagates backwards. Consequently, the wavelength of the wake initially increases with time until it becomes infinity and then starts to shrink until it can be damped. Besides, the phase velocity of the wake evolves in a similar way as the wavelength. The evolution of the wake results in heating of the plasma. Since the evolution of the wake depends on the local density gradient, an example of controlling the evolution process of the wake by tuning the initial density profile is given. The fast-evolving feature of the wakes may have the potential to be used as a new type of plasma based ultrafast photonic devices.

## Acknowledgments

This work was supported by NSFC Grant No. 11425521, No. 11375006, No. 11535006, No. 11475101, the National Basic Research Program of China No. 2013CBA01501, the US DOE Grant No. DE-SC0010064, No. DE-SC0008491, No. DE- SC0008316, No. DE-SC0014260, the US NSF Grant PHY-1415386, No. ACI-1339893 and No. PHY-500630, and the Ministry of Science and Technology of Taiwan under Contracts No. 104-2112-M-001-030 MY3. Simulations are performed on Hoffman cluster at UCLA and Edison cluster at National Energy Research Scientific Computing Centre (NERSC).

## ORCID iDs

C J Zhang https://orcid.org/0000-0001-8035-3014
F Li https://orcid.org/0000-0001-8627-910X
Y Wan https://orcid.org/0000-0001-6089-3718

## References

[1] Tajima T and Dawson J 1979 *Phys. Rev. Lett.* **43** 267–70
[2] Chen P, Dawson J, Huff R W and Katsouleas T 1985 *Phys. Rev. Lett.* **54** 693–6
[3] Mangles S *et al* 2004 *Nature* **431** 535–8
[4] Faure J, Glinec Y, Pukhov A, Kiselev S, Gordienko S, Lefebvre E, Rousseau J, Burgy F and Malka V 2004 *Nature* **431** 541–4
[5] Geddes C, Toth C, Tilborg J, Esarey E, Schroeder C, Bruhwiler D, Nieter C, Cary J and Leemans W 2004 *Nature* **431** 538–41
[6] Hogan M *et al* 2005 *Phys. Rev. Lett.* **95** 054802
[7] Blumenfeld I *et al* 2007 Energy doubling of 42 GeV electrons in a metre-scale plasma wakefield accelerator *Nature* **445** 741–4
[8] Corde S *et al* 2015 *Nature* **524** 442–5
[9] Blue B *et al* 2003 *Phys. Rev. Lett.* **90** 214801
[10] Corde S *et al* 2013 Femtosecond x rays from laser-plasma accelerators *Rev. Mod. Phys.* **85** 1
[11] Albert F *et al* 2014 Laser wakefield accelerator based light sources: potential applications and requirements *Plasma Phys. Control. Fusion* **56** 084015

[12] Phuoc T K *et al* 2012 All-optical Compton gamma-ray source *Nature Photonics* **6** 308–11
[13] Albert F *et al* 2013 Angular dependence of betatron x-ray spectra from a laser-wakefield accelerator *Phys. Rev. Lett.* **111** 235004
[14] Schroeder C, Esarey E, Geddes C, Benedetti C and Leemans W 2010 *Phys. Rev. Spec. Top.—Accel. Beams* **13** 101301
[15] Zhang C *et al* 2017 *Phys. Rev. Lett.* **119** 064801
[16] Sheng Z, Mima K, Zhang J and Sanuki H 2005 *Phys. Rev. Lett.* **94** 095003
[17] Fonseca R *et al* 2002 *OSIRIS: A Three-Dimensional, Fully Relativistic Particle in Cell Code for Modeling Plasma Based Accelerators* vol 2331 (Berlin: Springer) pp 342–51
[18] Dawson J 1961 On Landau Damping *Phys. of Fluids* **4** 869